

Bimolecular Homolytic Substitution (S_H2) at a Transition Metal

Ying Zhang,^[a] Kai-Dian Li,^[a] and Huan-Ming Huang^{*[a]}



Transition metal-catalyzed cross-coupling reactions have become a powerful and widely used synthetic approach for the construction of both carbon-carbon and carbon-heteroatom bonds. These reactions have revolutionized synthetic chemistry by enabling the efficient formation of complex molecular architectures. Among the various methods available, the bimolecular homolytic substitution (S_{H2}) reaction has emerged as an attractive and versatile method for the formation of $C(sp^3)-C(sp^3)$ and $C(sp^3)$ -heteroatom bonds. In recent years, significant progress has been made in the development of radical S_{H2} reactions, particularly those involving different

transition metal complexes such as cobalt, nickel, and iron. These advancements have expanded the scope of S_{H2} reactions, allowing for greater diversity in substrate compatibility and reaction conditions. In this review, we aim to highlight the latest breakthroughs and mechanistic insights into radical S_{H2} reactions, focusing on the role of transition metal catalysts in facilitating these transformations. We will discuss the various types of transition metal complexes that have been employed, the mechanistic pathways involved, and the potential applications of these reactions in the synthesis of complex organic molecules.

1. Introduction

Since the 2010 Nobel Prize in Chemistry highlighted the pivotal role of palladium-catalyzed cross-couplings in organic synthesis, there has been a significant surge in interest in transition-metal-catalyzed cross-coupling methods. These techniques have revolutionized synthetic strategies by enabling the efficient formation of diverse molecular architectures.^[1] Traditional approaches in this domain have predominantly focused on constructing $C(sp^2)-C(sp^2)$ and $C(sp^2)-X$ bonds, which are well-established in organic synthesis. However, the construction of $C(sp^3)-C(sp^3)$ and $C(sp^3)-X$ bonds has remained relatively underexplored, despite their importance in creating more complex and functionally diverse molecules.^[2-4]

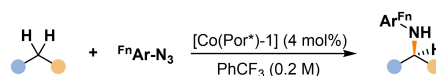
Bimolecular homolytic substitution (S_{H2}) is an fundamental step in radical chemistry.^[5-7] Notably, Davies and Roberts have provided an extensive review on bimolecular homolytic substitution at metal atoms, highlighting the mechanistic intricacies and the potential of this reaction type.^[8] Furthermore, Johnson's 1983 review on the bimolecular homolytic displacement of transition-metal complexes from carbon atoms has been instrumental in advancing our understanding of these processes.^[9] Pioneered by Kharasch,^[10] Fenton^[11] and Groves^[12], these foundational studies have clearly propelled the development of S_{H2} reactions within the realm of organometallic and synthetic chemistry.

Despite these advances, the integration of S_{H2} reactions with transition metal complexes has been relatively less explored by synthetic chemists.^[13] This underexplored area presents a significant opportunity, as combining S_{H2} mechanisms with transition metal catalysis could provide a robust synthetic approach for constructing $C(sp^3)-C(sp^3)$ and $C(sp^3)-X$ bonds.^[14] These bonds are crucial for the synthesis of many natural products, pharmaceuticals, and advanced materials, where the presence of sp^3 -hybridized centers often imparts desirable physical and chemical properties.^[15-17] Herein, we highlighted recent advances in bimolecular homolytic substitution (S_{H2}) involving transition metals, particularly focusing on cobalt, iron and nickel.

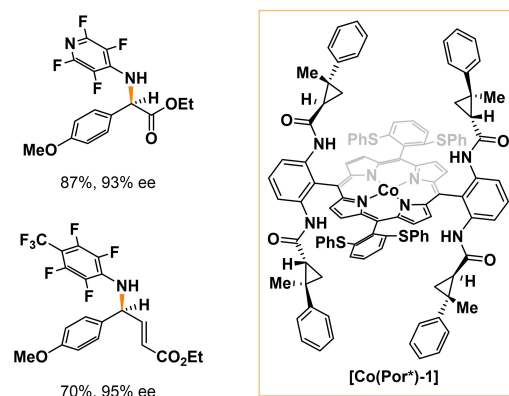
2. Bimolecular Homolytic Substitution (S_{H2}) at a Cobalt Complex

The vitamin B₁₂ derivative methylcobalamin, along with related methylcorrinoids, are fundamentally important organometallic cofactors in methylation reactions. In 2000, Krautler and co-workers reported that methyl-Co^{III} corrinoid cofactors are well-known to react with exogenous (R^*) to afford $R-CH_3$ via an S_{H2} reaction.^[18] This finding established a foundational understanding of the role of methylcorrinoids in radical-based methylation processes. Zhang and co-workers already demonstrated that

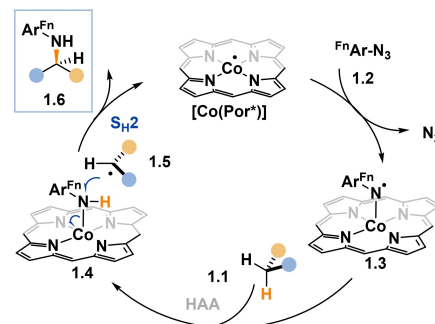
■ Zhang, 2020



Selected examples

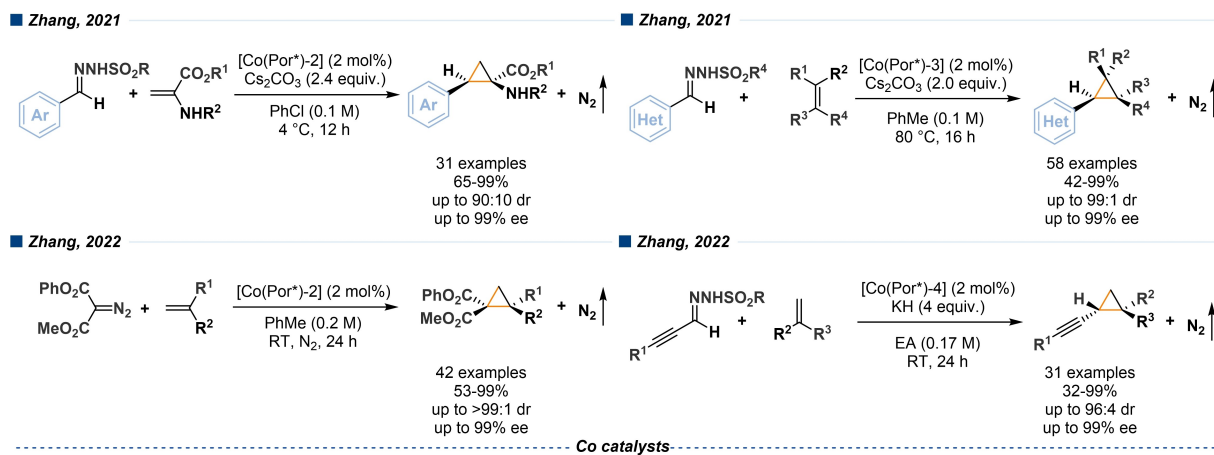


Plausible mechanism

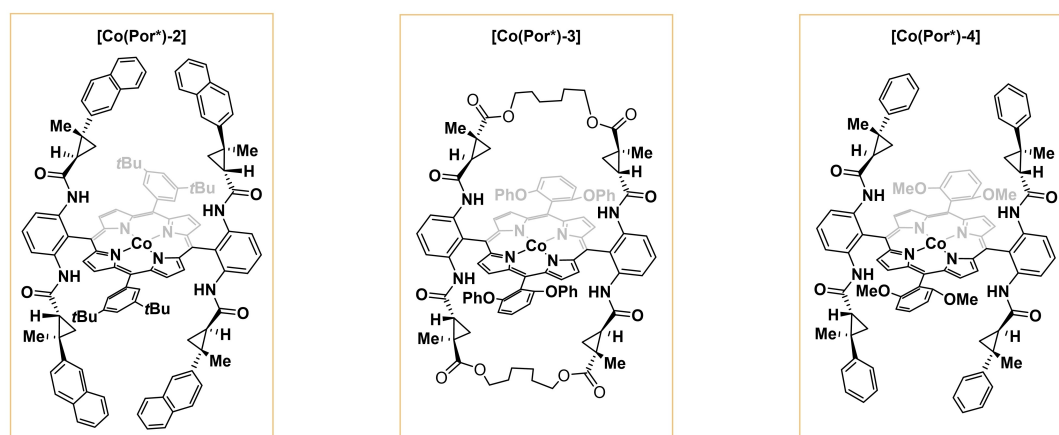


Scheme 1. Enantioselective intermolecular radical C–H amination.

[a] Y. Zhang, K.-D. Li, H.-M. Huang
School of Physical Science and Technology, ShanghaiTech University, 393
Middle Huaxia Road, Pudong, 201210 Shanghai, China
E-mail: huanghm@shanghaitech.edu.cn



Co catalysts

Scheme 2. Asymmetric radical cyclopropanation involving radical S_H2 reaction.

the cobalt(II) complexes of porphyrins [Co(Por)] has appeared as efficient metalloradical catalysts, capable of facilitating a wide range of synthetic transformations that involve S_H2 reaction.^[19,20]

These cobalt(II) porphyrin complexes have been shown to enable diverse and highly selective reactions, expanding the utility of S_H2 mechanisms in modern synthetic chemistry. For



Ying Zhang received her B.Sc. degree from University of Shanghai for Science and Technology. From 2021, she started the graduate study under the supervision of Prof. Huan-Ming Huang in School of Physical Science and Technology at ShanghaiTech University. Her research interests focus on metallaphotoredox chemistry.

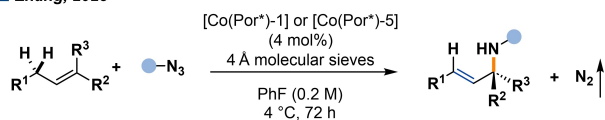


Huan-Ming Huang received his Ph.D. under the direction of Professor David J. Procter at The University of Manchester (U.K.). Then he continued to stay in the same group as an EPSRC postdoctoral fellow. In 2018, he joined the group of Professor Frank Glorius at the University of Münster (Germany) as an Alexander von Humboldt postdoctoral research fellow. Later in 2021, he started his independent career as an assistant professor (tenure track) in the School of Physical Science and Technology (SPST), ShanghaiTech University (China). Currently, his main research interests focus on the development of energy transfer catalysis and asymmetric radical chemistry.

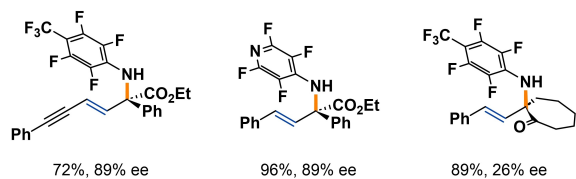


Kai-Dian Li received his B.Sc. from the South China Agricultural University. In 2023, he started his Master's degree under the supervision of Prof. Huan-Ming Huang at the School of Physical Science and Technology at ShanghaiTech University. His research interests focus on dual photoredox and transition metal catalysis.

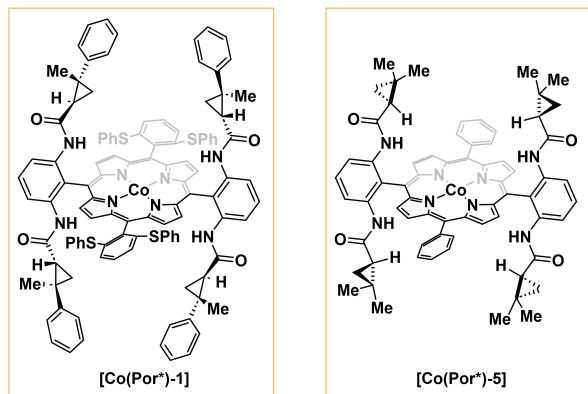
Zhang, 2023



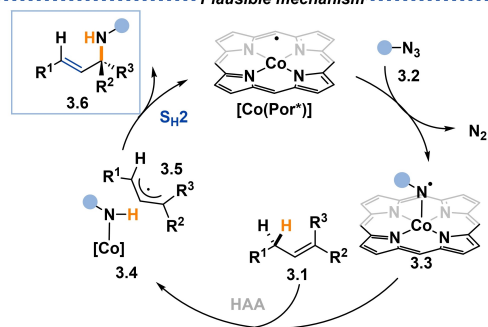
Selected examples



Co catalysts

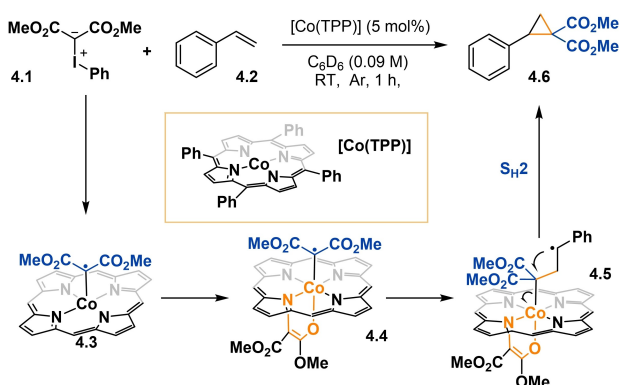


Plausible mechanism



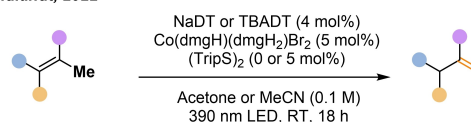
Scheme 3. Enantioselective intermolecular radical allylic C–H amination.

de Bruin, 2022

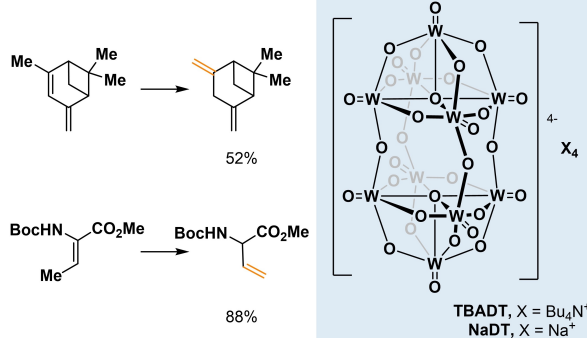


Scheme 4. Cobalt(II) catalyzed carbene transfer from ylide.

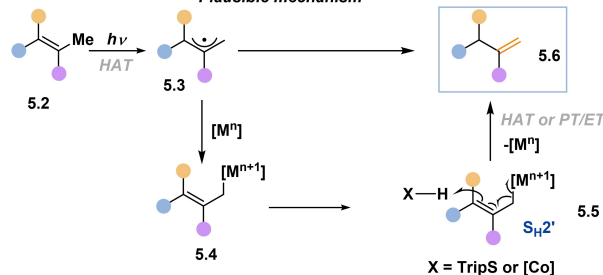
Wendlandt, 2022



Selected examples



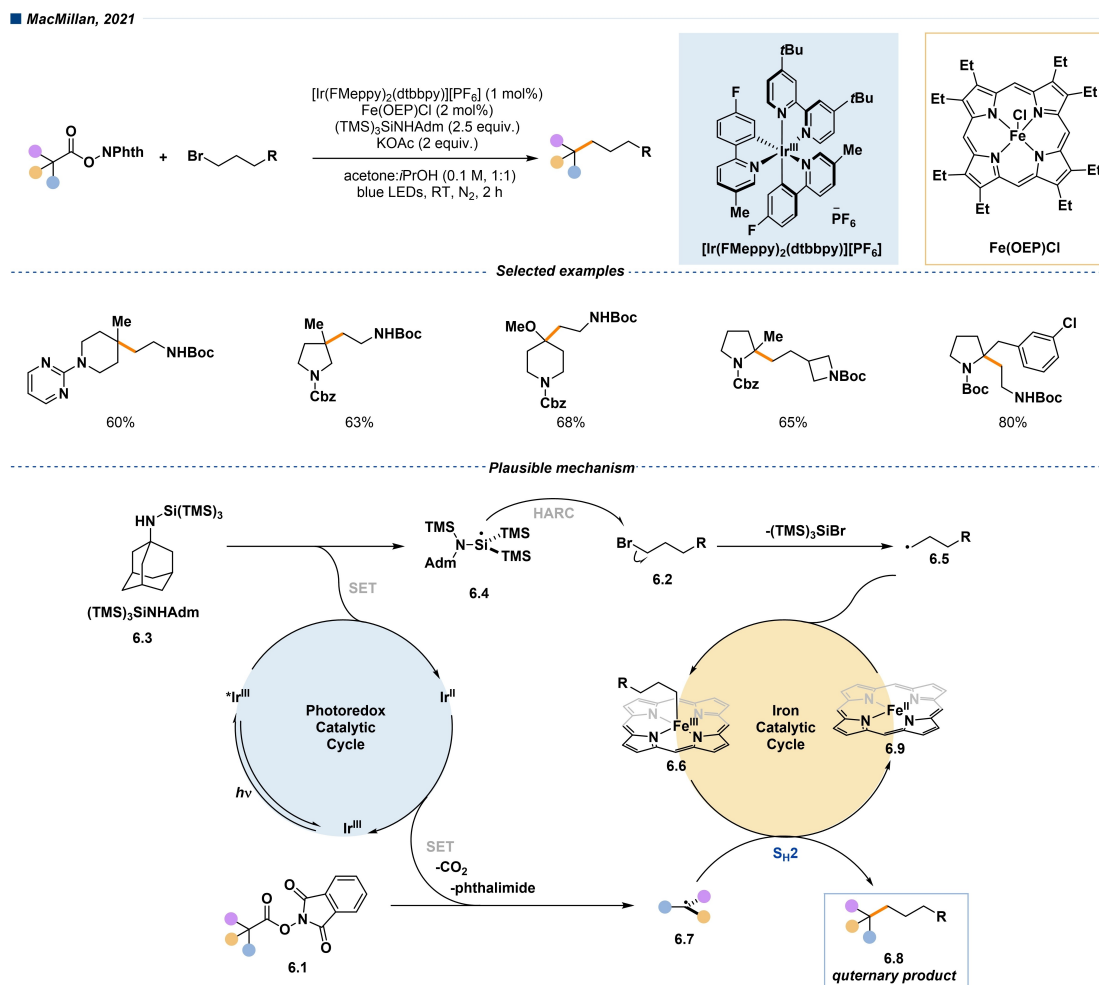
Plausible mechanism

Scheme 5. Catalytic, *contra*-thermodynamic positional alkene isomerization.

example, Zhang and co-workers demonstrated an impressive example of enantioselective intermolecular radical C–H amination involving a radical S_{H2} reaction to construct the C–N bond (Scheme 1).^[21] In this process, organic azides are reduced by chiral porphyrins [Co(Por)] to form the corresponding nitrogen centered radical 1.3. Following hydrogen atom abstraction (HAA) between the hydrocarbon substrate 1.1 and nitrogen centered radical 1.3, the newly generated benzylic radical 1.5 could react with the chiral cobalt intermediate 1.4, producing chiral amine motifs 1.6 through a radical S_{H2} reaction.

Later on, Zhang and his team achieved several elegant examples of asymmetric radical cyclopropanation involving a radical S_{H2} reaction to construct the C–C bond (Scheme 2).^[22,23] They successfully synthesized a variety of three-membered ring motifs, including chiral cyclopropyl α -amino acids,^[24] chiral heteroaryl cyclopropane,^[25] chiral 1,1-cyclopropanediester,^[26] and chiral alkynyl cyclopropanes.^[27] These syntheses were accomplished through sequential radical generation, addition and S_{H2} to close the ring with high yield and selectively.

Very recently, Zhang and co-workers demonstrated an enantioselective intermolecular radical allylic C–H amination using a Co(II)-based metalloradical catalysis (Scheme 3).^[28] As they proposed, the nitrogen centered radical 3.3 is generated from the interaction between organic azide 3.1 and a chiral Co(II) catalyst. Following an intermolecular hydrogen atom abstraction (HAA) step between 3.3 and 3.1, the newly formed allylic radical 3.5 undergoes a radical S_{H2} reaction with 3.4,



Scheme 6. A biomimetic $S_{\text{H}2}$ cross-coupling mechanism for quaternary sp^3 -carbon formation

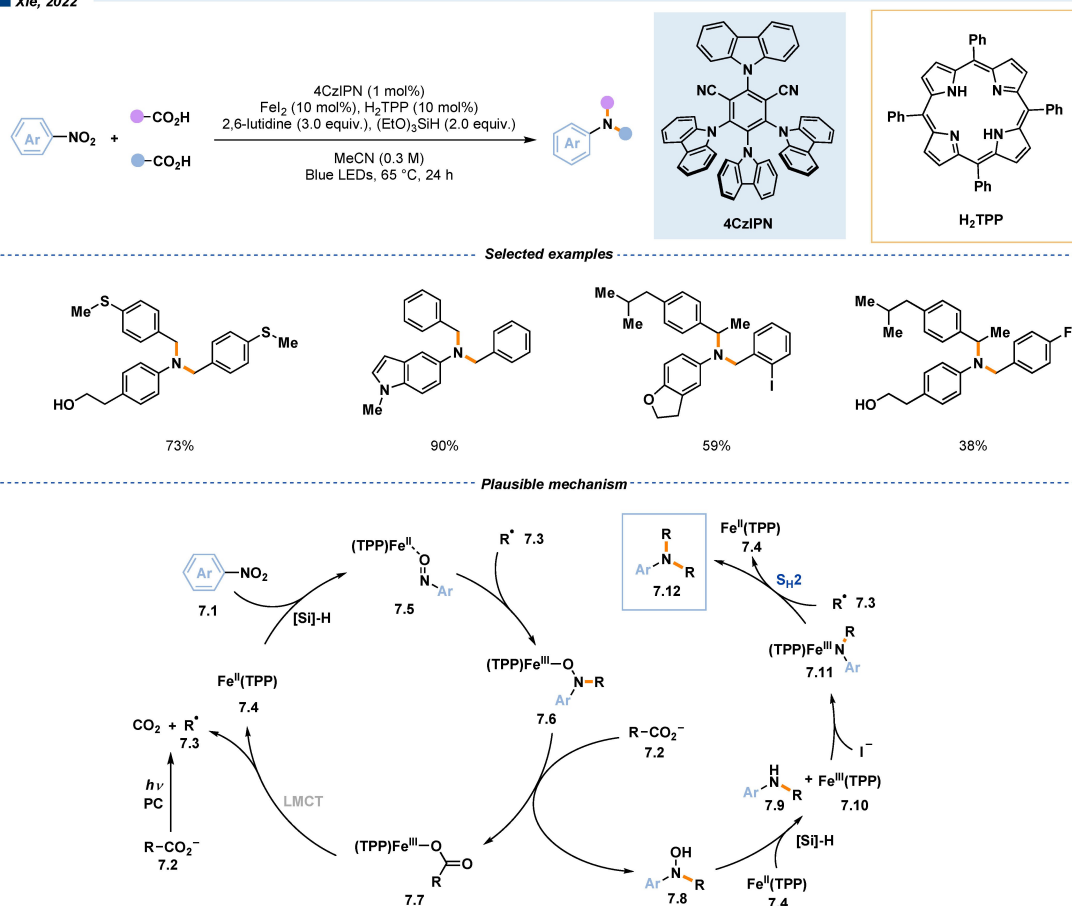
resulting in the formation of chiral allylic amines **3.6** with high yields and excellent enantioselectivity. Impressively, the catalytic system demonstrates a high tolerance for isomeric mixtures of alkenes, effectively converting them into valuable chiral α -tertiary amines. This highlights the robustness and versatility of the Co(II)-based metalloradical catalysis approach in achieving enantioselective transformations.

In 2022, de Bruin and co-workers achieved a cross coupling reaction between iodonium ylides **4.1** and styrene **4.2** using a catalytic amount of cobalt catalysis (Scheme 4).^[29,30] They proposed that a disubstituted cobalt(III) radical **4.3** could be derived from a cobalt(II)-tetraphenylporphyrin complex and iodonium ylide **4.1**, which serves as a carbene precursor. The cobalt(III) radical **4.3** could react with another equivalent of iodonium ylides **4.1** to generate intermediate **4.4**. This intermediate subsequently reacts with styrene **4.2** to form the radical intermediate **4.5**. The cyclopropane product **4.6** is efficiently generated through a radical $S_{\text{H}2}$ reaction. The innovative approach of using iodonium ylides as carbene precursors in combination with cobalt catalysis opens new avenues for the construction of cyclopropane rings, which are

valuable structures in medicinal chemistry and materials science.

In 2022, Wendlandt and co-workers successfully achieved photochemical *contra*-thermodynamic positional alkene isomerization with a regioselective bimolecular homolytic substitution ($S_{\text{H}2}'$) as a key step (Scheme 5).^[31] They devised a dual catalytic system by combining tungsten catalysts and cobalt catalysts, enabling terminal-selective alkenes to be obtained with a broad scope. The innovative approach involved sequential hydrogen atom abstraction, allylic cobalt formation, and $S_{\text{H}2}'$ reaction to promote *contra*-thermodynamic internal-to-terminal olefin isomerization. By merging tungsten and cobalt catalysts, Wendlandt and her team were able to orchestrate regioselective transformations, achieving high levels of selectivity and efficiency. The ability to control the regioselectivity of alkene isomerization through the strategic use of dual catalysis represents a significant advancement in the field of alkene functionalization.

Xie, 2022

Scheme 7. Decarboxylative tandem C–N coupling with nitroarenes via S_{H2} mechanism.

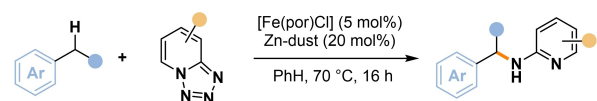
3. Bimolecular Homolytic Substitution (S_{H2}) at an Iron Complex

In 2021, MacMillan and co-workers successfully achieve a biomimetic approach to $C(sp^3)–C(sp^3)$ cross coupling enabled by dual photoredox and iron catalysis (Scheme 6).^[32] Selective alkyl-alkyl cross-coupling has long remained a challenging goal in synthetic chemistry, and the authors addressed this challenge with their innovative strategy. The authors employed iridium-based photoredox catalyst to oxidize the silane reagent **6.3**, generating a silicon radical intermediate **6.4**; Subsequent halogen atom abstraction (XAT) between **6.4** and primary alkyl bromide **6.2** led to the formation of primary radical intermediate **6.5** efficiently. This primary radical intermediate **6.5** was then captured by the Fe(II) porphyrin catalyst at near diffusion controlled rates to furnish 1° alkyl-Fe(III) intermediate **6.6**. Simultaneously, the reduced iridium-based catalyst efficiently reduced **6.1** to generate tertiary radical **6.7**, which could further react with Fe(III) porphyrin catalyst **6.6** to form the final product **6.8** containing a quaternary carbon through a radical S_{H2} reaction. This biomimetic approach showcases the synergistic effects of dual photoredox and iron catalysis in achieving selective alkyl-alkyl cross-coupling. The strategic use of both catalysts allows for efficient generation and manipulation of

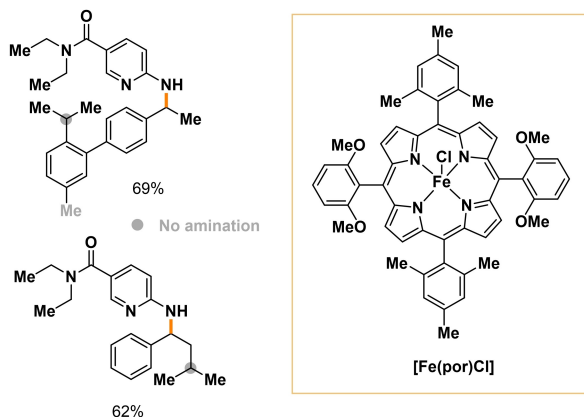
radical intermediates, facilitating the formation of challenging $C(sp^3)–C(sp^3)$ bonds with high efficiency and selectivity. The successful implementation of this strategy not only addresses a long-standing challenge in synthetic chemistry but also provides valuable insights into the design of catalytic systems for complex transformations. By mimicking the reactivity of biological systems, MacMillan and co-workers have expanded the synthetic toolbox available to chemists, offering new opportunities for the synthesis of complex organic molecules with diverse applications.

Soon after, Xie, Zhu, and co-workers reported an elegant example of decarboxylative tandem C–N coupling between carboxylic acid and nitroarenes through a radical S_{H2} reaction (Scheme 7).^[33] Under visible light conditions, enabled by dual photoredox and iron catalysis, a variety of aromatic tertiary amines could be obtained in good to excellent yields. Notably, the synthesis of nonsymmetric aromatic tertiary amines was also achieved by tolerating two different carboxylic acids, albeit in moderate yields. In their proposed mechanism, nitro compounds **7.1** could be reduced by the (TPP)Fe(II) catalyst in the presence of $(EtO)_3SiH$ to form Fe-based complexes **7.5**. These complexes could then be trapped by the alkyl radical intermediate **7.3** to afford intermediate **7.6**. Following anion exchange, the newly formed hydroxylamine compound **7.8**

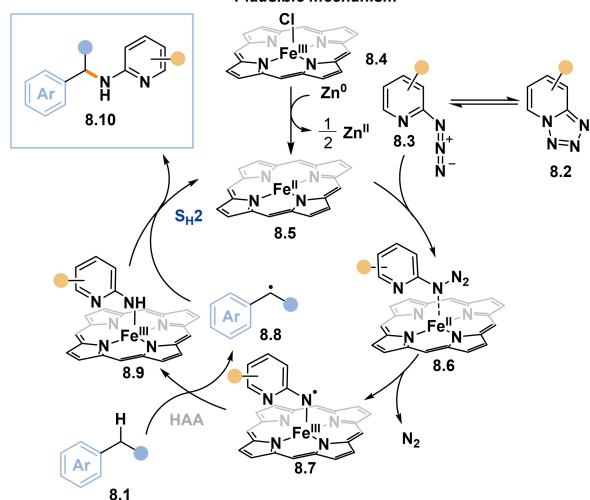
■ Chattopadhyay, 2022



Selected examples



Plausible mechanism

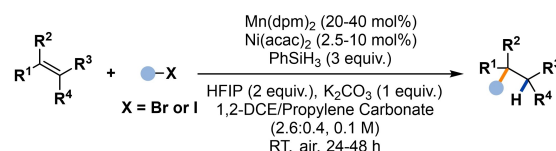


Scheme 8. Iron-catalyzed intermolecular amination of benzylic C(sp³)-H bonds.

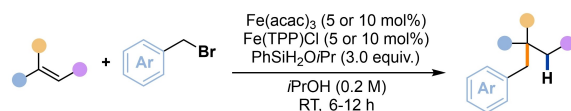
reacts with the (TPP)Fe(II) catalyst to form the amine compound 7.9, which combines with (TPP)Fe(III) catalyst to generate the (TPP)Fe(III) intermediate 7.11. Subsequently, a radical S_H2 reaction occurs between the alkyl radical 7.3 and the (TPP)Fe(III) complex 7.11, facilitating efficient formation of the final C-N bond production of the desired tertiary amine architectures. This innovative methodology not only showcases the potential of decarboxylative tandem coupling reactions for the synthesis of complex molecules but also highlights the versatility of dual photoredox and iron catalysis in enabling challenging transformations under mild conditions. The successful synthesis of aromatic tertiary amines, including nonsymmetric derivatives, underscores the practical utility of this approach in accessing structurally diverse and biologically relevant compounds.

In 2022, Chattopadhyay and his team demonstrated a catalytic system for intermolecular benzylic C(sp³)-H amination utilizing 1,2,3,4-tetrazole as a nitrene precursor via iron catalysis

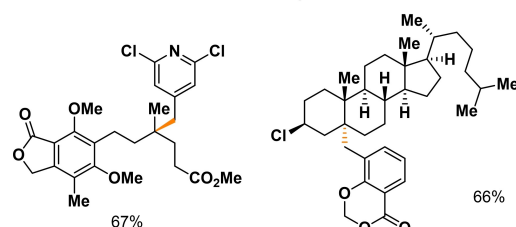
■ Shenvi, 2019



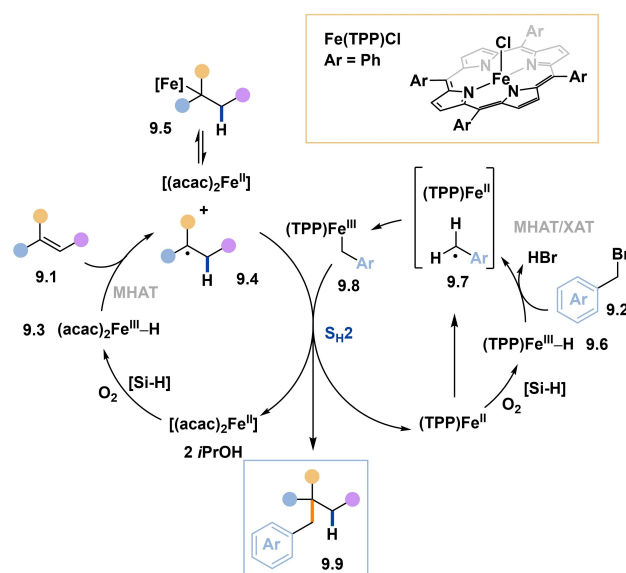
■ Shenvi, 2023



Selected examples



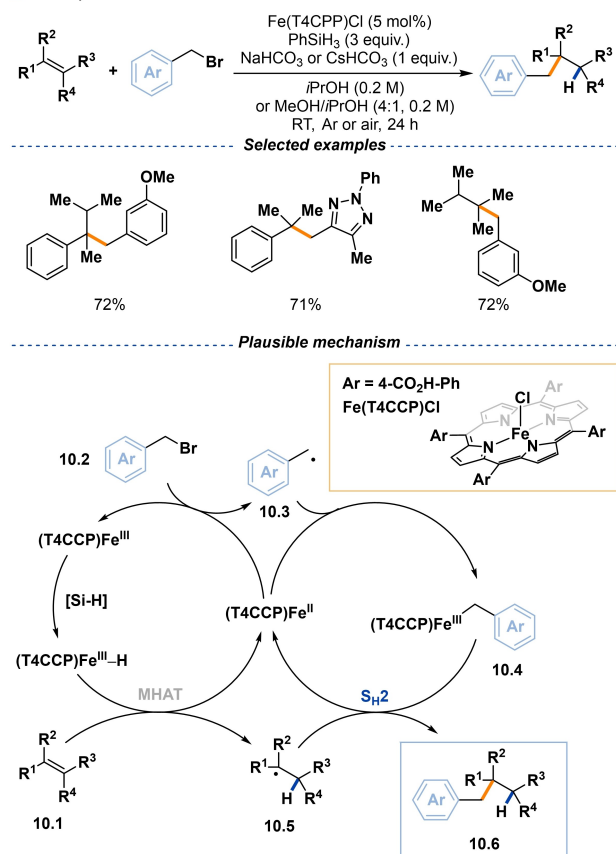
Plausible mechanism



Scheme 9. Iron-catalyzed hydrobenzylation of olefins via radical S_H2 reaction.

(Scheme 8).^[34] The innovative method selectively aminates secondary benzylic C(sp³)-H bond over tertiary and primary benzylic C(sp³)-H bonds, showcasing remarkable regioselectivity. The broad substrate scope of this open-shell approach has been exemplified in the synthesis of Dapoxetine, highlighting its synthetic utility. In their proposed mechanism, the iron(II)-porphyrin catalyst is generated in situ by the mixture of zinc and iron(III)-porphyrin. This iron(II)-porphyrin species then reacts with tetrazole 8.2 to form a nitrogen-centered radical intermediate 8.7. This electrophilic radical 8.7 selectively reacts with the benzylic C-H bond to generate benzylic radical 8.8. Following this step, a radical S_H2 reaction occurs between the benzylic radical 8.8 and the nitrogen-centered radical intermediate 8.9, resulting in the efficient formation of the final amine product 8.10. This sequence of reactions allows for the

Shenvi, 2024



Scheme 10. Iron catalyzed cross-coupling between styrenes and benzyl bromides.

regioselective introduction of an amino group at the desired position, providing access to valuable amine derivatives with high efficiency. The development of this catalytic system represents a significant advancement in the field of C–H functionalization, particularly in the selective functionalization of benzylic C(sp³)–H bonds. By harnessing the reactivity of nitrogen-centered radicals derived from tetrazole, Chattopadhyay and his team have expanded the synthetic toolbox for the construction of complex molecular architectures.

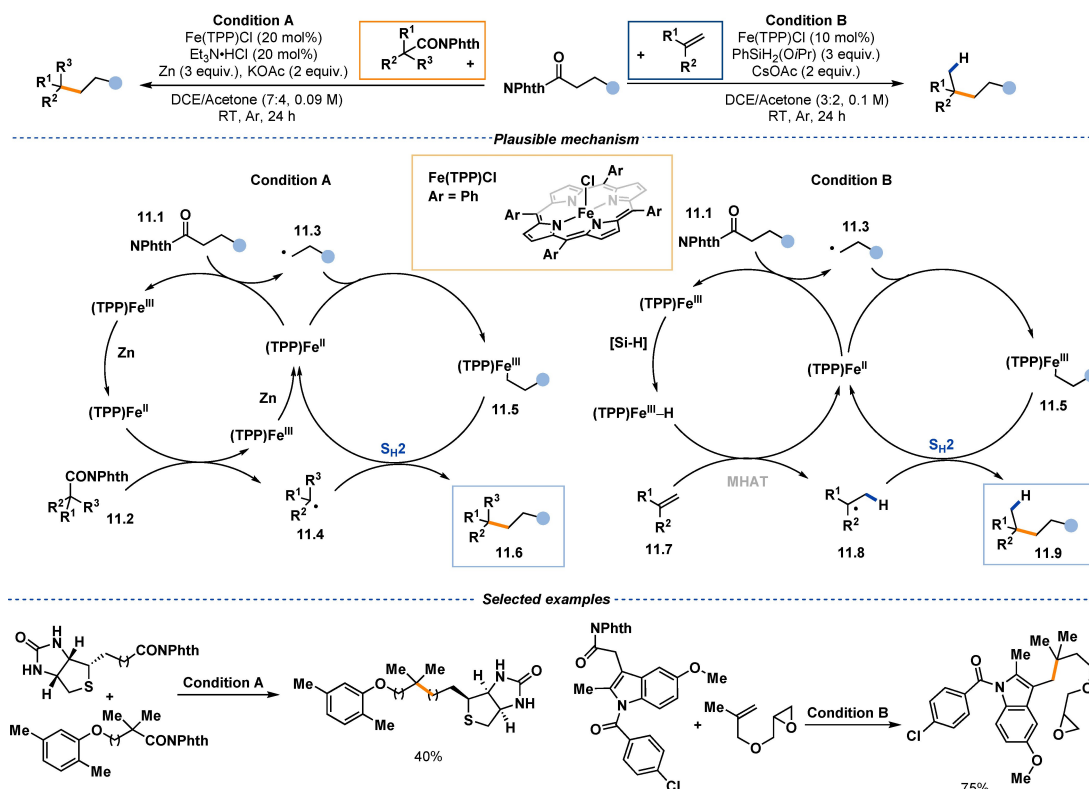
In 2023, Shenvi and co-workers successfully merged metal-hydride hydrogen atom transfer (MHAT)^[35] with a radical S_H2 reaction to achieve iron-catalyzed hydrobenzylation of unactivated olefins (Scheme 9).^[36] This innovative strategy enables the synthesis of a variety of products containing a quaternary center in high yield. The synthetic approach exhibits broad substrate scope and has been applied in the stereoselective synthesis of (–)-eugenol. In their breakthrough study, radical intermediate **9.4** is formed through iron catalyzed MHAT with an alkene. Concurrently, benzylic radical **9.7** could be generated through HAT or XAT steps. This benzylic radical **9.7** is then trapped by an iron(II) intermediate to form an iron(III) complex. The key radical S_H2 step between the tertiary radical **9.4** and the iron complex **9.8** leads to the formation of the quaternary center, enabling efficient hydrobenzylation of unactivated olefins. Furthermore, the same research group

successfully utilized a single iron catalyst to achieve the cross-coupling reaction between styrenes and benzyl bromides through a key S_H2 step (Scheme 10).^[37] They identified an iron porphyrin catalyst [Fe(T4CCP)Cl] as effective in cross-coupling alkenes with benzyl bromides via radical intermediates, even when two benzyl radicals of similar stability are formed as intermediates. Remarkably, the coupling scope includes mono-, di-, tri-, and tetrasubstituted alkenes among conjugated and unconjugated alkenes alike. This open-shell approach represents a powerful platform in the synthesis of complex architectures and the modification of natural products. By harnessing the reactivity of radical intermediates and leveraging the versatility of iron catalysis, Shenvi and his team have expanded the synthetic toolbox for the construction of structurally diverse molecules.

Very recently, Shenvi, Baran, and Kawamata reported a general platform for constructing an all-carbon quaternary center between redox active esters and olefins through decarboxylative coupling (Scheme 11).^[38] In this innovative approach, they successfully discovered that an iron(tetraphenylporphyrinato) chloride [Fe(TPP)Cl] catalyzes two different redox-active esters, enabling the efficient formation of coupled products containing an all-carbon quaternary center. Notably, they applied this methodology in the synthesis of complex architectures and natural products, offering simpler synthetic routes. In their proposed mechanism, [Fe(TPP)Cl] catalysis, in combination with silane, forms an iron hydride that reacts with alkenes **11.3** to generate radical intermediate **11.7**. Concurrently, the reduced iron catalyst reduces the redox-active ester **11.1** to form the primary radical **11.4**. Following a radical S_H2 reaction, the final product **11.8** is efficiently formed from the primary radical and tertiary radical intermediates. This method represents a significant advancement in the field of decarboxylative coupling reactions, enabling the efficient construction of all-carbon quaternary centers. By leveraging the reactivity of redox-active esters and the versatility of iron catalysis, Shenvi, Baran, and Kawamata have provided a powerful tool for the synthesis of structurally diverse molecules with complex architectures.

In 2023, MacMillan and his team employed tertiary alcohols and alkyl halides to the synthesis of sterically congested quaternary products enabled by dual photoredox and iron catalyst (Scheme 12).^[39] This radical approach demonstrates a relatively broad substrate scope with good yields, making it a valuable tool for synthetic chemists. Furthermore, they applied their method efficiently in the synthesis of complex architectures, showcasing its synthetic versatility and utility. In their innovative approach, the authors utilized benzoxazolium salt (NHC) to activate the alcohol **12.1**, forming intermediate **12.3**. With the aid of a suitable photoredox catalyst, the tertiary radical intermediate **12.5** is efficiently formed. Concurrently, the reduced photoredox catalyst reduces the silane reagent **12.6** to abstract the halogen atom of alkyl bromide **12.2** to generate alkyl radical **12.8**, which is then trapped by the iron (II) catalyst to form an iron (III) intermediate. Finally, the tertiary radical intermediate **12.5** reacts with the alkyl radical intermediate **12.9** to produce the final product **12.10**, regenerating the iron (II)

Baran & Shenvi, 2024



Scheme 11. Carbon quaternization of redox active esters and olefins by decarboxylative coupling.

catalyst in the process. This cascade of reactions highlights the synergistic effects of dual photoredox and iron catalysis in enabling the efficient construction of sterically congested quaternary products from simple starting materials.

In 2023, Zhang and co-workers developed five-coordinate iron(III) complexes of porphyrins with an axial ligand and used them as a new type of metalloradical catalysis for the synthesis of chiral cyclopropanes (Scheme 13).^[40] Their innovative approach enabled the cyclopropanation reaction between styrenes and α -trifluoromethyldiazomethanes or diazo compounds using catalytic amounts of [Fe(Por)Cl], resulting in the formation of a variety of chiral trifluoromethyl-substituted cyclopropane in high yields with excellent enantioselectivity. In their proposed mechanism, the iron(III) catalyst could react with substrate 13.3 to generate iron(IV) catalyst 13.4, which subsequently reacts with styrene 13.2 to form the alkyl radical 13.5. Following an intramolecular S_{H2} reaction, the intermediate 13.5 undergoes cyclization to yield the chiral product 13.6. Simultaneously, the iron(III) catalyst is regenerated, completing the catalytic cycle. This elegant strategy highlights the utility of metalloradical catalysis in enabling complex transformations with high efficiency and selectivity.

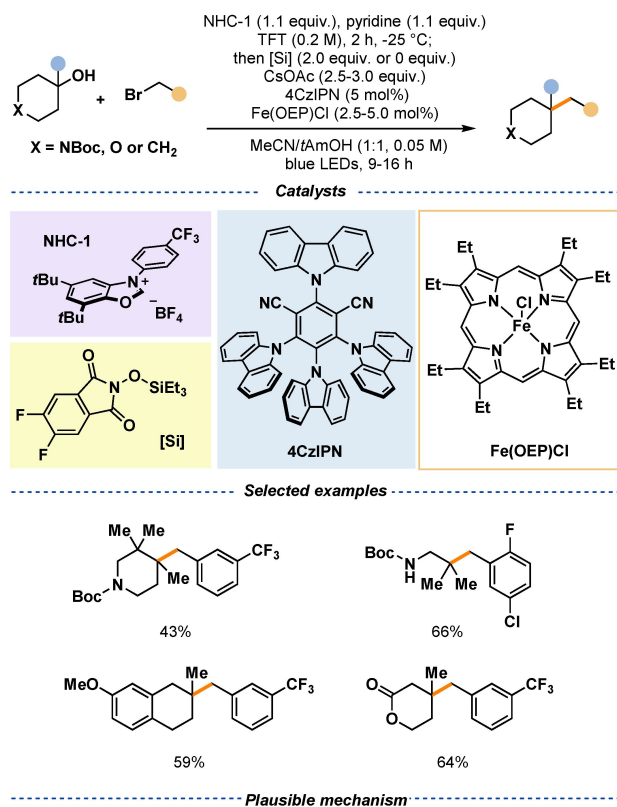
In 2022, West^[41] and Shi^[42] independently reported elegant diazidation of alkenes enabled by iron catalysis (Scheme 14). These innovative works offer a mild, efficient, acid-free approach of diazidation of unactivated alkenes via ligand-to-metal charge transfer (LMCT) / S_{H2} process. The plausible mechanism demonstrates that azide anion is trapped by iron(III)

and is then excited by visible light to get azide radical 14.4 through LMCT process, azide radical 14.4 react with unactivated alkene 14.1 to generate tertiary radical intermediate 14.5. After the S_{H2} process between tertiary radical intermediate 14.5 and iron intermediate 14.2, the final diazidation product could be formed efficiently.

Following their previous work, West and co-workers successfully developed a method of decarboxylative azidation of unactivated alkyl carboxylic acids directly through LMCT/ S_{H2} process (Scheme 15).^[43] In this innovative approach, cheap and easy-accessible trimethylsilyl azide was used as the azide source to get the direct azidation product from alkyl carboxylic acids. In their proposed mechanism, alkyl carboxylic acid 15.1 cooperates with ferric nitrate 15.2 to form iron intermediate 15.3, after excitation by purple light, going through the process of LMCT, alkyl radical intermediate 15.5 is generated after the elimination of CO_2 . Then, the iron(II) is oxidized by nitrate and thus cooperates with azide anion to generate iron intermediate 15.9. Finally, alkyl radical intermediate 15.5 undergoes an S_{H2} process with iron intermediate 15.9 to get the final product 15.11.

Recently, Koh, Zhang and Holland reported an elegant example regarding regioselective functionalization of olefins with sp^3 -hybridized organohalides and organozinc reagents using a simple (terpyridine)iron catalyst (Scheme 16).^[44] The method grants access to a range of valuable $C(sp^3)$ -rich molecules, which are notoriously difficult to synthesize, including alicyclic compounds featuring multiple adjacent stereo-

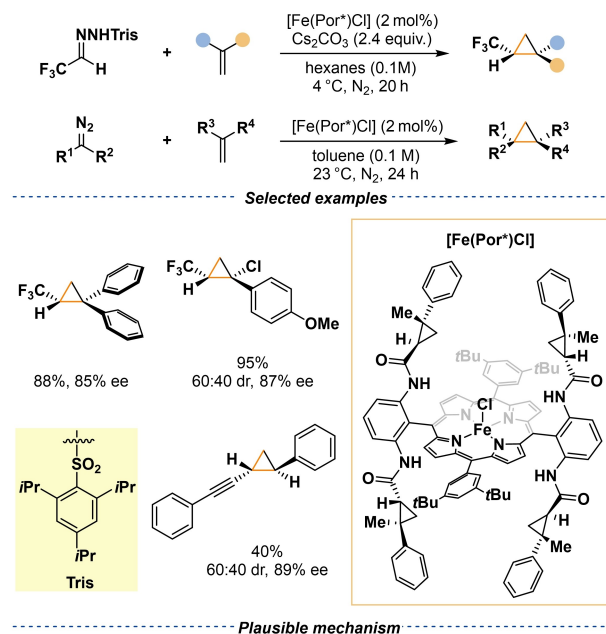
MacMillan, 2023



Scheme 12. Synthesis of sterically congested quaternary products via S_H2 reaction.

centers, via annulation cascades. Based on the mechanistic studies and computational studies, they proposed that iron catalyst could react with organozinc reagent **16.3** and alkyl halide **16.2** to form iron (II) intermediate **16.7**, which then react with alkenes **16.1** to form intermediate **16.8**. The newly formed alkyl radical **16.6** then attacks the iron (II) intermediate **16.8** to form the final coupling product **16.9**, while the iron (I) complex is formed efficiently. The active iron (I) complex **16.4** could react

Zhang, 2023

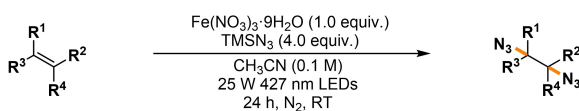


Scheme 13. Iron(III)-based metalloradical catalysis for asymmetric cyclopropanation.

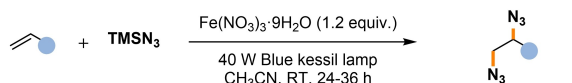
with organozinc reagent **16.3** and alkyl halide **16.2** to regenerate iron(II) complex **16.7**.

In 2024, Yang and co-workers reported an elegant example of enantioselective construction of quaternary stereocenters via cooperative photoredox/Fe/chiral primary amine triple catalysis (Scheme 17).^[45] This innovative approach represents a significant advancement in the field of catalytic asymmetric synthesis, offering a versatile strategy for the synthesis of chiral cyclic compounds containing a quaternary stereocenter with high yields and excellent enantioselectivities. In their proposed mechanism, cyclic ketone **17.1** reacts with a chiral primary amine to form imine intermediate **17.3**. This imine intermediate undergoes single-electron transfer (SET) oxidation to generate tertiary radical intermediate **17.4**. Concurrently, the reduced photoredox catalyst reduces the redox-active ester **17.2** to form the primary radical intermediate **17.5**. Furthermore, the primary radical intermediate **17.5** could be trapped by iron(II) catalyst to form iron(III) catalyst **17.6**. This iron(III) catalyst then reacts with

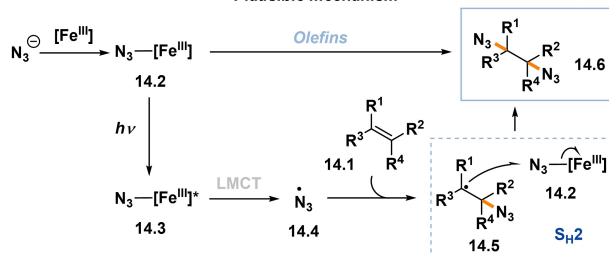
■ West, 2022



■ Shi, 2022

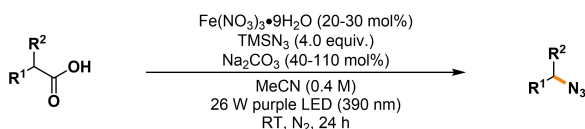


Plausible mechanism

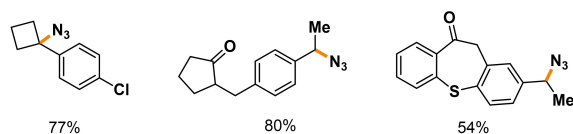


Scheme 14. Diazidation of alkenes enabled by iron catalysis.

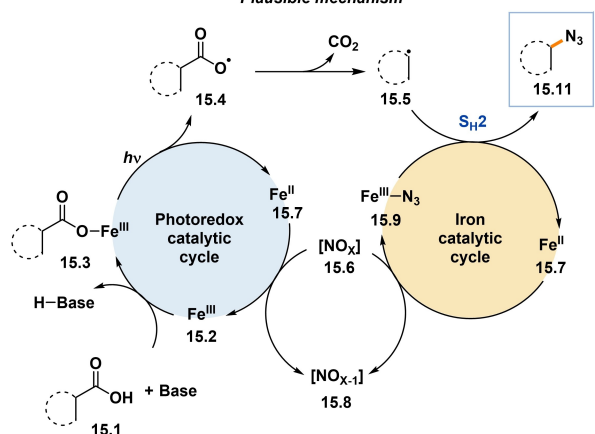
■ West, 2023



Selected examples



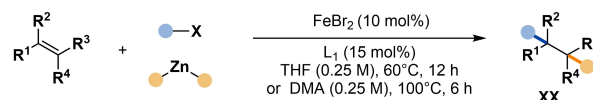
Plausible mechanism



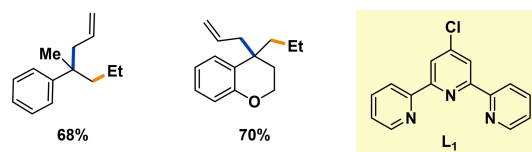
Scheme 15. Decarboxylative azidation of unactivated alkyl carboxylic acids.

radical intermediate **17.4** to construct the quaternary center intermediate **17.7** efficiently. Upon releasing the primary amine catalyst, the desired product **17.8** is formed efficiently, completing the catalytic cycle.

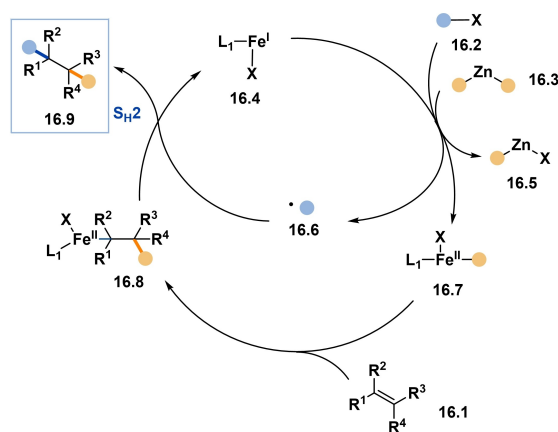
■ Koh, 2024



Selected examples



Plausible mechanism



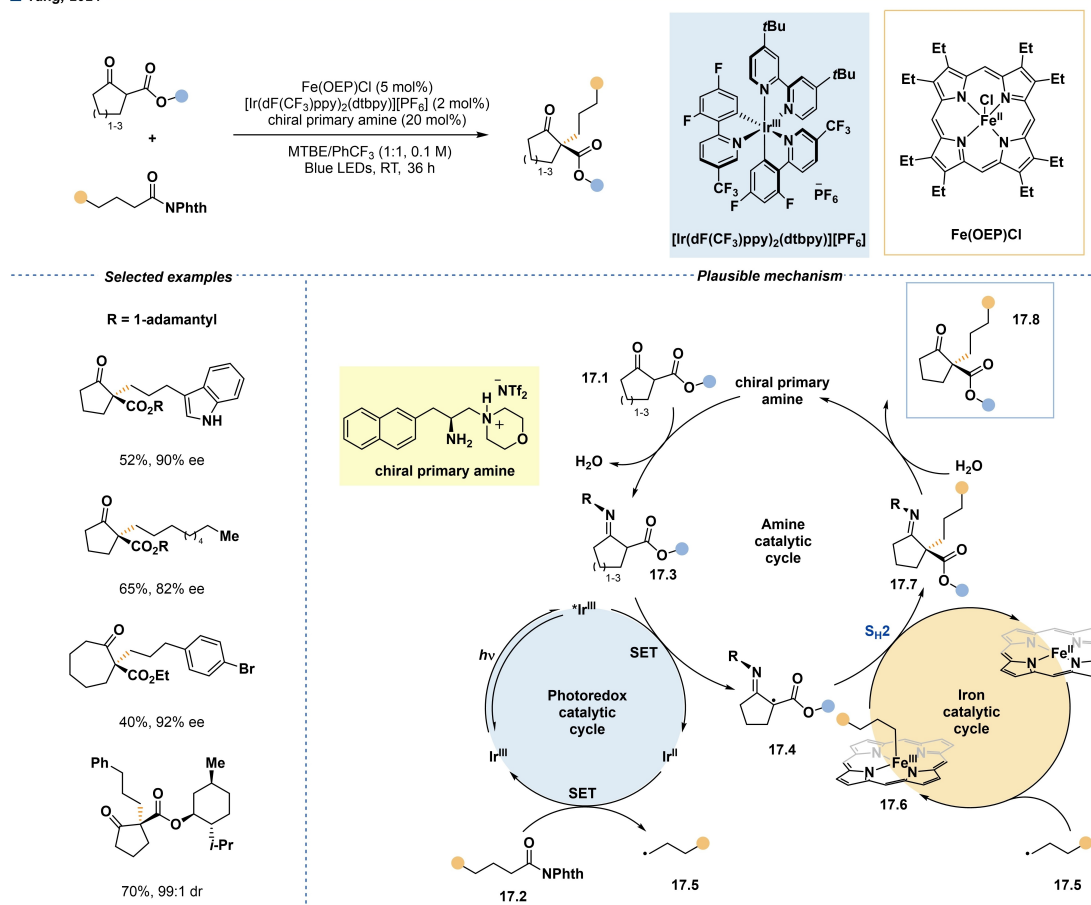
Scheme 16. Dialkylation of alkenes enabled by iron catalysis.

4. Bimolecular Homolytic Substitution (S_{H2}) at a Nickel Complex

In 2019, Sanford and colleagues demonstrated that Ni(IV) complexes could react with peroxide to form carbon-carbon bond formation through S_{H2} reaction (Scheme 18).^[46] They successfully demonstrated that Ni(III) complex could react with methyl radical to form Ni(IV) complex, which could be attacked by another alkyl radical which generated in situ from peroxide precursor. They proposed that this key carbon-carbon bond formation is achieved by the radical S_{H2} reaction. Their groundbreaking study showcased the capability of Ni(III) complexes to react with methyl radicals, leading to the formation of Ni(IV) complexes. Subsequently, these Ni(IV) complexes were susceptible to attack by alkyl radicals, which were generated in situ from peroxide precursors. This mechanism elucidates how the pivotal carbon-carbon bond formation occurs through radical S_{H2} reaction, highlighting the significance of metal-mediated radical processes in organometallic chemistry.

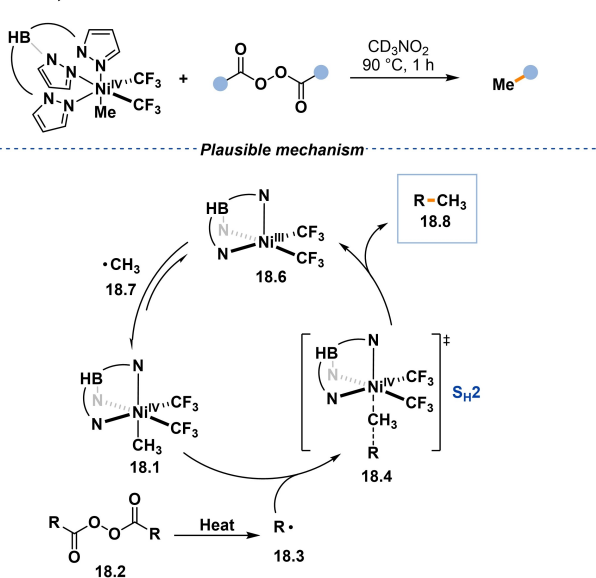
In 2022, the MacMillan group achieved the decarboxylative cross-coupling of two carboxylic acids via a dual photoredox/nickel catalytic platform, utilizing radical S_{H2} reaction as a key step (Scheme 19).^[47] Their groundbreaking work demonstrated the successful utilization of two different aliphatic carboxylic acids to facilitate valuable C(sp³)-C(sp³) bond formation with a broad substrate scope. In their proposed mechanism, a mixture

■ Yang, 2024



Scheme 17. Enantioselective construction of quaternary stereocenters via cooperative photoredox/Fe/chiral primary amine triple catalysis.

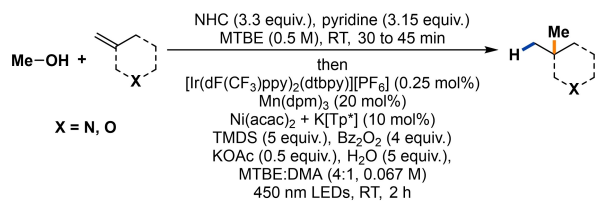
■ Sanford, 2019

Scheme 18. S_{H2} reaction between carbon-centered radicals with high-valent organonickel complexes.

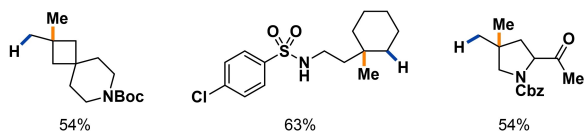
of $Mes_2(OAc)_2$ and two different aliphatic acids leads to the formation of hypervalent iodine intermediate 19.3. This intermediate is activated by a suitable photocatalyst through an energy transfer mechanism, generating two different alkyl radical intermediates, 19.4 and 19.5. The less sterically hindered radical intermediate, 19.4, is trapped by Ni(II) complex to form Ni(III) intermediate 19.6. Subsequently, a radical S_{H2} reaction occurs between 19.6 and alkyl radical intermediate 19.5, leading to the efficient formation of the desired product 19.9. Meanwhile, the nickel (II) complex is regenerated, completing the catalytic cycle. The broad substrate scope and efficiency of this method underscore its potential utility in synthetic chemistry and its significance in advancing the field of radical-mediated cross-coupling reactions.

In 2024, MacMillan and his team successfully demonstrated the late-stage $C(sp^3)-H$ methylation of drug molecules by merging decatungstate photocatalysis with nickel-mediated S_{H2} bond formation (Scheme 20).^[48] This innovative method has been effectively applied in modifying complex drugs with high yields, offering a versatile strategy for late-stage functionalization. In their proposed mechanism, radical intermediate 20.3 is efficiently formed through a hydrogen atom abstraction (HAA) step between hydrocarbon 20.1 and decatungstate photocatalysis. Concurrently, the redox-active ester 20.2 is reduced to

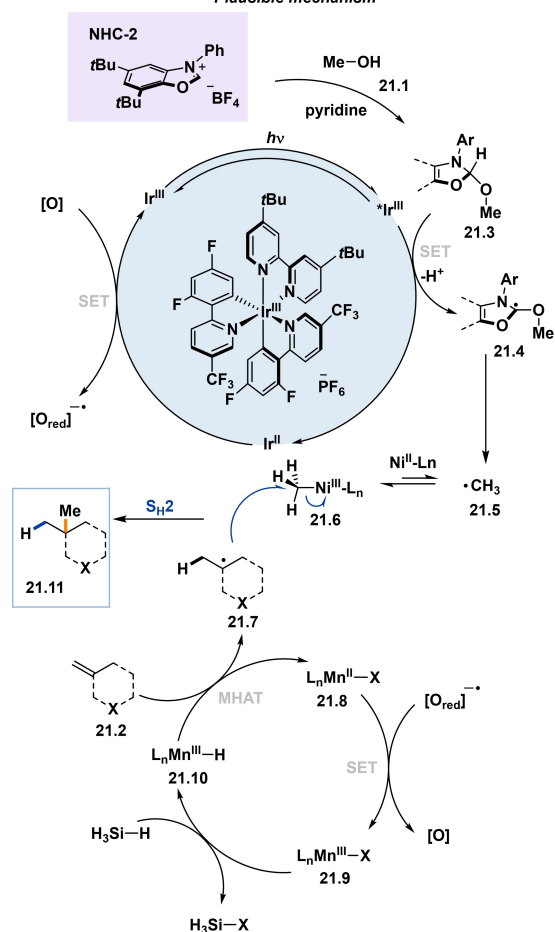
MacMillan, 2024



Selected examples



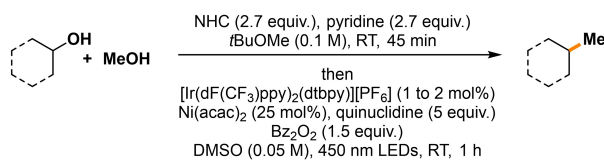
Plausible mechanism



Scheme 21. A triple catalytic, radical sorting approach to olefin-alcohol cross-coupling.

In the same year, MacMillan and co-workers achieved alcohol-alcohol cross-coupling enabled by $\text{S}_{\text{H}2}$ radical coupling (Scheme 22).^[50] Compared to previous methods, they successfully utilized two different alcohols, both activated by N-heterocyclic carbene (NHC) species, to form alkyl radical intermediates. With the assistance of a Ni(II) complex, these two alkyl radicals underwent coupling to form the carbon-carbon bond. This innovative approach offers a versatile strategy for the synthesis of complex molecules through the direct coupling

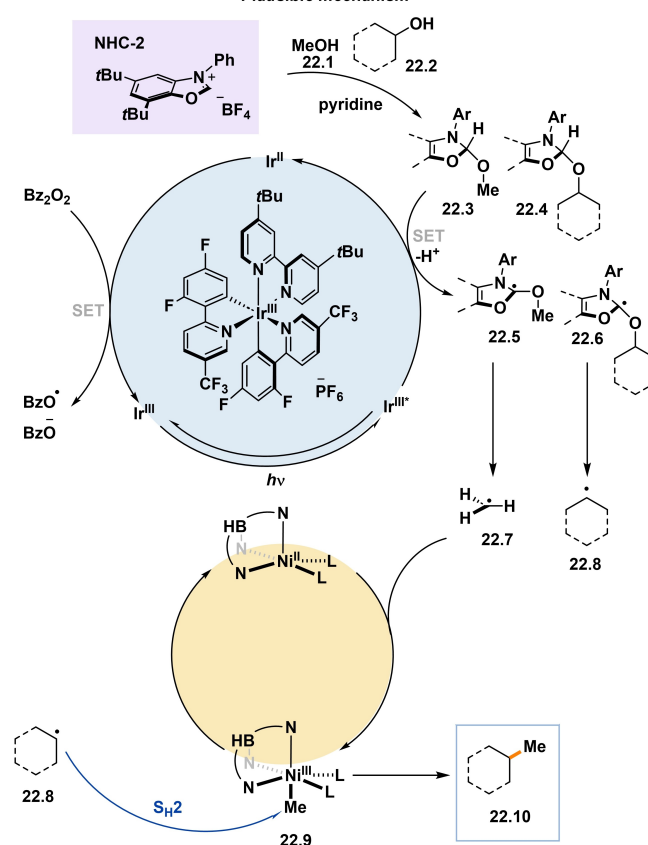
MacMillan, 2024



Selected examples



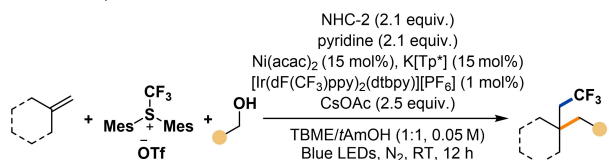
Plausible mechanism

Scheme 22. Alcohol-alcohol cross-coupling enabled by $\text{S}_{\text{H}2}$ reaction.

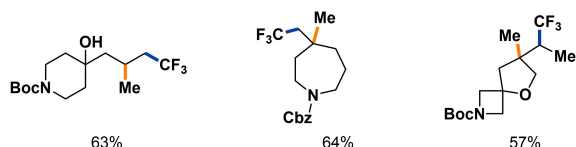
of alcohol substrates, expanding the scope of radical-mediated cross-coupling reactions.

Very recently, the MacMillan group expanded their reaction from two-component cross-coupling to three-component coupling (Scheme 23).^[51] By employing radical $\text{S}_{\text{H}2}$ reaction as a key step, they successfully achieved the simultaneous construction of two $\text{C}(\text{sp}^3)-\text{C}(\text{sp}^3)$ bonds. The substrate scope of this methodology is relatively broad, exhibiting excellent functional group tolerance under mild reaction conditions. In their proposed mechanism, primary radical species **23.6** is generated through sequential NHC activation, single-electron transfer (SET) oxidation, and β -scission. Simultaneously, the trifluoromethyl radical **23.7** could be formed by the reduced photocatalysis, which are

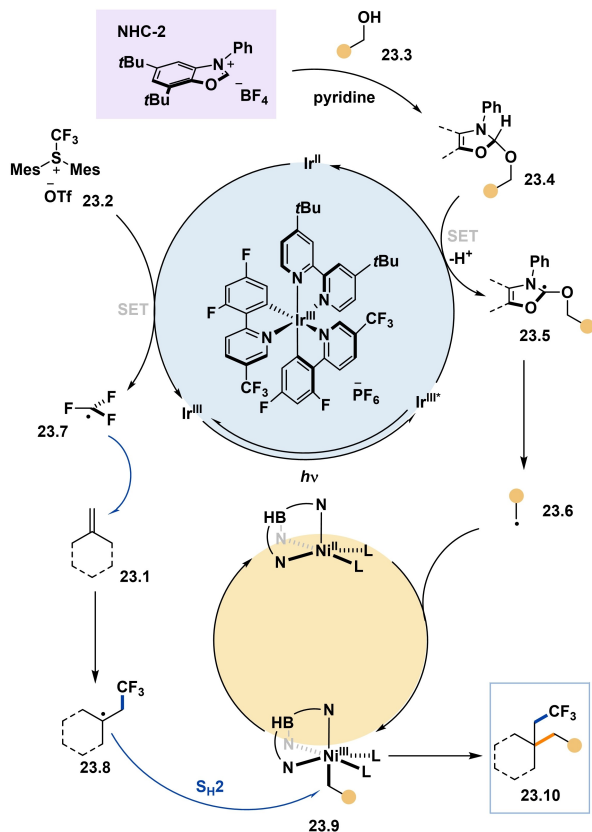
MacMillan, 2024



Selected examples



Plausible mechanism

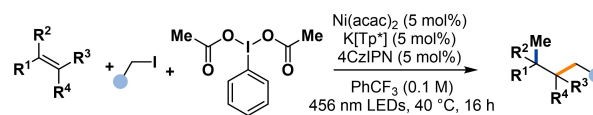


Scheme 23. Alkene dialkylation by triple radical sorting.

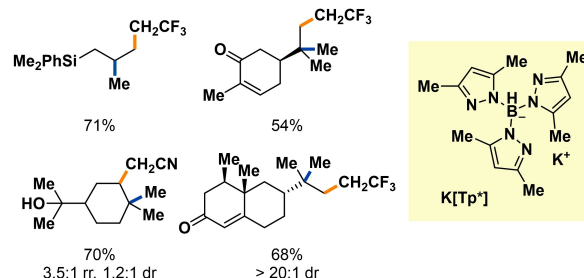
rapidly trapped by the unactivated alkene **23.1** to form the tertiary radical intermediate **23.8**. With the aid of a Ni(II) complex, the primary radical species **23.6** couples with the tertiary radical intermediate **23.8** to efficiently form the complex architecture **23.10**.

In the meantime, Koh and co-workers developed an elegant photoredox/nickel dual catalytic approach to form two C(sp³)–C(sp³) linkages via trimolecular cross-coupling of alkenes with alkyl halides and hypervalent iodine-based reagents. (Scheme 24).^[52] This method demonstrated excellent tolerance to a variety of functional groups and natural product-based scaffolds, with the corresponding products obtained in high yields. In their proposed mechanism, the photoexcited photo-

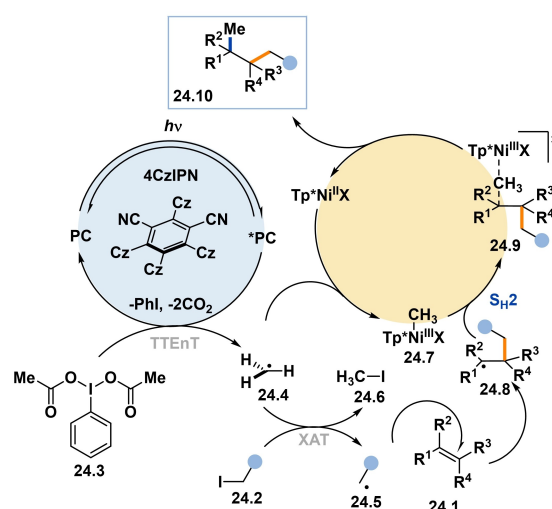
Koh, 2024



Selected examples

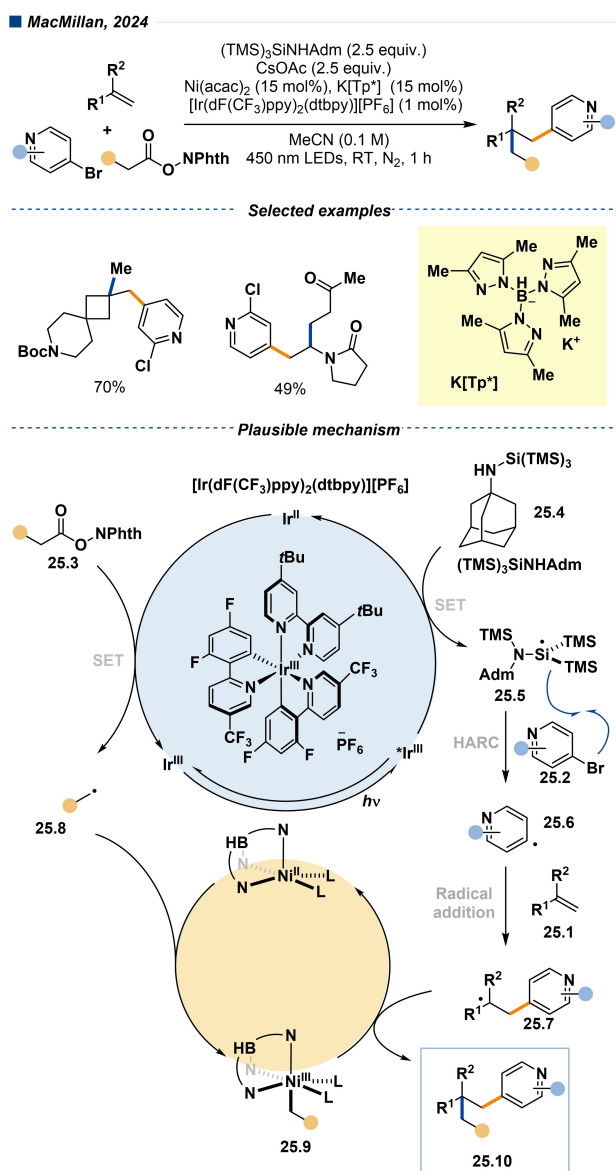


Plausible mechanism

Scheme 24. Multicomponent cross-coupling of unactivated alkenes via S_H2 reaction.

catalyst activates the hypervalent iodine compound **24.3** to generate methyl radical **24.4** via an energy-transfer mechanism. This methyl radical then reacts with iodine compound **24.2** to generate alkyl radical **24.5**. Meanwhile, another equivalent of methyl radical is trapped by a Ni(II) complex to form Ni(III) intermediate **24.7** efficiently. Subsequently, alkyl radical **24.5** adds to alkenes to generate more stable radical intermediate **24.8**, which then reacts with Ni(III) complex successfully to construct the three-component coupling product **24.10**.

In their continued exploration of multicomponent reactions involving S_H2 reactions, MacMillan and co-workers successfully achieved the aryl-alkylation of alkenes involving aryl radical intermediates (Scheme 25).^[53] They utilized aryl halides, redox-active esters, and unactivated alkenes as coupling partners, producing the coupling product with high yields. In their proposed mechanism, they employed silane reagent **25.4** to abstract the halogen from aryl halide **25.2**, efficiently forming the corresponding aryl radical **25.6**. This aryl radical then adds to the unactivated alkene efficiently to generate the secondary radical intermediate **25.7**. Concurrently, the primary radical

Scheme 25. Aryl-alkylation of alkenes via S_{H2} reaction.

25.8 reacts with a Ni(II) complex to form the corresponding Ni(III) intermediate 25.9. The key step involves the reaction of the secondary radical intermediate 25.7 with the Ni(II) intermediate 25.9, leading to the formation of the final coupled product 25.10 via an S_{H2} reaction. This innovative method broadens the scope of multicomponent coupling reactions, providing a versatile and efficient strategy for constructing complex molecular architectures from readily available starting materials. The ability to form aryl-alkylated products in high yields showcases the potential of this approach in synthetic organic chemistry, particularly for the rapid synthesis of functionalized molecules with diverse applications.

5. Summary and Outlook

In recent years, significant studies have explored the development of radical S_{H2} reactions for forming $C(sp^3)-C(sp^3)$ and $C(sp^3)-X$ bonds. We highlight the concept of radical S_{H2} reactions and their application in merging S_{H2} reactions with various transition metal catalysis, including cobalt, iron, and nickel. This approach demonstrates that bimolecular homolytic substitution (S_{H2}) at a transition metal can serve as a general synthetic platform for constructing saturated architectures. Future directions and opportunities including 1) Expansion to Other Transition Metals: The merging of S_{H2} reactions with different transition metal catalysis is poised for further development. Beyond cobalt, iron, and nickel, exploring other transition metals such as copper,^[54–56] manganese,^[57] and chromium could uncover new reactivity patterns and broaden the scope of S_{H2} reactions. This could lead to the discovery of novel catalytic systems with unique selectivities and efficiencies; 2) Development of asymmetric methodologies: asymmetric synthetic approaches involving radical S_{H2} steps could become a general platform for constructing chiral $C(sp^3)-C(sp^3)$ and $C(sp^3)-X$ bonds. These methodologies would be particularly valuable in the synthesis of enantiomerically pure compounds, which are crucial in pharmaceuticals and agrochemicals. The design of chiral ligands and catalysts tailored for S_{H2} reactions will be a key area of research; 3) Application in complex molecule synthesis: applying S_{H2} -based methodologies to the late-stage functionalization of complex molecules and natural products can provide more efficient and selective routes to these valuable compounds. This approach could simplify synthetic routes, reduce the number of steps required, and improve overall yields, making it an attractive strategy for the synthesis of bioactive molecules and natural products; 4) Multicomponent and tandem reactions: The development of multicomponent and tandem reactions involving S_{H2} steps can streamline the synthesis of complex molecules. By combining multiple transformations in a single reaction sequence, chemists can construct intricate molecular architectures more efficiently. This strategy could be particularly useful in drug discovery and development, where rapid access to diverse compound libraries is essential; 5) Integration with photoredox and electrochemical catalysis: The integration of S_{H2} reactions with photoredox and electrochemical catalysis offers exciting opportunities for developing new synthetic methodologies. These approaches can enable the generation of radical intermediates under mild conditions and provide precise control over reaction pathways. This combination could lead to the discovery of novel reactivity and expand the utility of S_{H2} reactions in organic synthesis.

The integration of radical S_{H2} reactions with transition metal catalysis represents a powerful and versatile approach in modern synthetic chemistry. Continued exploration and development in this area promise to deliver innovative solutions for constructing complex, functionalized molecules with precision and efficiency. As the field progresses, the merging of S_{H2} reactions with other catalytic strategies and the development of asymmetric methodologies will significantly expand the toolkit

of synthetic chemists, providing new opportunities for creating valuable compounds in various domains of chemistry.

Acknowledgements

We are grateful for financial support from the National Natural Science Foundation of China (22201179 to H.-M. H.).

Conflict of Interests

The authors declare no conflict of interest.

Keywords: S_H2 reaction · Radicals · Transition metals · Cross-coupling · Bimolecular homolytic substitution

- [1] C. C. C. Johansson Seechurn, M. O. Kitching, T. J. Colacot, V. Snieckus, *Angew. Chem. Int. Ed.* **2012**, *51*, 5062–5085.
- [2] J. Choi, G. C. Fu, *Science* **2017**, *356*, eaaf7230.
- [3] E. Geist, A. Kirschning, T. Schmidt, *Nat. Prod. Rep.* **2014**, *31*, 441.
- [4] C. P. Johnston, R. T. Smith, S. Allmendinger, D. W. C. MacMillan, *Nature* **2016**, *536*, 322–325.
- [5] K. U. Ingold, B. P. Roberts, *Free-Radical Substitution Reactions: Bimolecular Homolytic Substitutions (Sh₂ Reactions) at Saturated Multivalent Atoms*, John Wiley & Sons, Inc, Hoboken, NJ **1971**.
- [6] A. L. J. Beckwith, *Tetrahedron* **1981**, *37*, 3073–3100.
- [7] C. H. Schiesser, L. M. Wild, *Tetrahedron* **1996**, *52*, 13265–13314.
- [8] A. G. Davies, B. P. Roberts, *Nat. Phys.* **1971**, *229*, 221–223.
- [9] M. D. Johnson, *Acc. Chem. Res.* **1983**, *16*, 343–349.
- [10] M. S. Kharasch, G. Sosnovsky, N. C. Yang, *J. Am. Chem. Soc.* **1959**, *81*, 5819–5824.
- [11] Z. Tang, P. Zhao, H. Wang, Y. Liu, W. Bu, *Chem. Rev.* **2021**, *121*, 1981–2019.
- [12] X. Huang, J. T. Groves, *JBC J. Biol. Inorg. Chem.* **2017**, *22*, 185–207.
- [13] D. T. Nemoto, K.-J. Bian, S.-C. Kao, J. G. West, *Beilstein J. Org. Chem.* **2023**, *19*, 1225–1233.
- [14] J. C. Walton, *Acc. Chem. Res.* **1998**, *31*, 99–107.
- [15] F. Lovering, J. Bikker, C. Humblet, *J. Med. Chem.* **2009**, *52*, 6752–6756.
- [16] J. Boström, D. G. Brown, R. J. Young, G. M. Keserü, *Nat. Rev. Drug Discovery* **2018**, *17*, 709–727.
- [17] K. R. Campos, P. J. Coleman, J. C. Alvarez, S. D. Dreher, R. M. Garbaccio, N. K. Terrett, R. D. Tillyer, M. D. Truppo, E. R. Parmee, *Science* **2019**, *363*, eaat0805.
- [18] H. Mosimann, B. Kräutler, *Angew. Chem. Int. Ed.* **2000**, *39*, 393–395.
- [19] W. C. C. Lee, X. P. Zhang, *Angew. Chem. Int. Ed.* **2024**, *63*, e202320243.
- [20] H.-M. Huang, M. H. Garduño-Castro, C. Morrill, D. J. Procter, *Chem. Soc. Rev.* **2019**, *48*, 4626–4638.
- [21] L.-M. Jin, P. Xu, J. Xie, X. P. Zhang, *J. Am. Chem. Soc.* **2020**, *142*, 20828–20836.
- [22] X. Wang, X. Peter Zhang, in *Transit. Met. Carbene Transform.*, Wiley **2022**, 25–66.
- [23] W.-C. C. Lee, X. P. Zhang, *Trends Chem.* **2022**, *4*, 850–851.
- [24] W.-C. C. Lee, D.-S. Wang, C. Zhang, J. Xie, B. Li, X. P. Zhang, *Chem* **2021**, *7*, 1588–1601.
- [25] X. Wang, J. Ke, Y. Zhu, A. Deb, Y. Xu, X. P. Zhang, *J. Am. Chem. Soc.* **2021**, *143*, 11121–11129.
- [26] J. Wang, J. Xie, W.-C. Cindy Lee, D.-S. Wang, X. P. Zhang, *Chem. Catal.* **2022**, *2*, 330–344.
- [27] J. Ke, W. C. C. Lee, X. Wang, Y. Wang, X. Wen, X. P. Zhang, *J. Am. Chem. Soc.* **2022**, *144*, 2368–2378.
- [28] P. Xu, J. Xie, D.-S. Wang, X. P. Zhang, *Nat. Chem.* **2023**, *15*, 498–507.
- [29] R. F. J. Epping, M. M. Hoeksma, E. O. Bobylev, S. Mathew, B. de Bruin, *Nat. Chem.* **2022**, *14*, 550–557.
- [30] D. D. Snabilić, E. J. Meeus, R. F. J. Epping, Z. He, M. Zhou, B. de Bruin, *Chem. A Eur. J.* **2023**, *29*, e202300336.
- [31] G. Occhialini, V. Palani, A. E. Wendlandt, *J. Am. Chem. Soc.* **2022**, *144*, 145–152.
- [32] W. Liu, M. N. Lavagnino, C. A. Gould, J. Alcázar, D. W. C. MacMillan, *Science* **2021**, *374*, 1258–1263.
- [33] S. Wang, T. Li, C. Gu, J. Han, C.-G. Zhao, C. Zhu, H. Tan, J. Xie, *Nat. Commun.* **2022**, *13*, 2432.
- [34] H. Khatua, S. Das, S. Patra, S. K. Das, S. Roy, B. Chattopadhyay, *J. Am. Chem. Soc.* **2022**, *144*, 21858–21866.
- [35] S. L. Shevick, C. V. Wilson, S. Kotesova, D. Kim, P. L. Holland, R. A. Shenvi, *Chem. Sci.* **2020**, *11*, 12401–12422.
- [36] X. C. Gan, S. Kotesova, A. Castanedo, S. A. Green, S. L. B. Møller, R. A. Shenvi, *J. Am. Chem. Soc.* **2023**, *145*, 15714–15720.
- [37] L. Kong, X. C. Gan, V. A. van der Puyl Lovett, R. A. Shenvi, *J. Am. Chem. Soc.* **2024**, *146*, 2351–2357.
- [38] X. C. Gan, B. Zhang, N. Dao, C. Bi, M. Pokle, L. Kan, M. R. Collins, C. C. Tyrol, P. N. Bolduc, M. Nicastrì, Y. Kawamata, P. S. Baran, R. Shenvi, *Science* **2024**, *384*, 113–118.
- [39] C. A. Gould, A. L. Pace, D. W. C. MacMillan, *J. Am. Chem. Soc.* **2023**, *145*, 16330–16336.
- [40] W.-C. C. Lee, D.-S. Wang, Y. Zhu, X. P. Zhang, *Nat. Chem.* **2023**, *15*, 1569–1580.
- [41] K.-J. Bian, S.-C. Kao, D. Nemoto, X.-W. Chen, J. G. West, *Nat. Commun.* **2022**, *13*, 7881.
- [42] M. Zhang, J. Zhang, Q. Li, Y. Shi, *Nat. Commun.* **2022**, *13*, 7880.
- [43] S.-C. Kao, K.-J. Bian, X.-W. Chen, Y. Chen, A. A. Martí, J. G. West, *Chem Catal.* **2023**, *3*, 100603.
- [44] T.-D. Tan, J. M. I. Serviano, X. Luo, P.-C. Qian, P. L. Holland, X. Zhang, M. J. Koh, *Nat. Catal.* **2024**, *7*, 321–329.
- [45] L. J. Li, J. C. Zhang, W. P. Li, D. Zhang, K. Duanmu, H. Yu, Q. Ping, Z. P. Yang, *J. Am. Chem. Soc.* **2024**, *146*, 9404–9412.
- [46] J. R. Bour, D. M. Ferguson, E. J. McClain, J. W. Kampf, M. S. Sanford, *J. Am. Chem. Soc.* **2019**, *141*, 8914–8920.
- [47] A. V. Tsymbal, L. D. Bizzini, D. W. C. Macmillan, *J. Am. Chem. Soc.* **2022**, *144*, 21278–21286.
- [48] E. Mao, D. W. C. MacMillan, *J. Am. Chem. Soc.* **2023**, *145*, 2787–2793.
- [49] Q. Cai, I. M. McWhinnie, N. W. Dow, A. Y. Chan, D. W. C. MacMillan, *J. Am. Chem. Soc.* **2024**, *146*, 12300–12309.
- [50] R. Chen, N. E. Intermaggio, J. Xie, J. A. Rossi-Ashton, C. A. Gould, R. T. Martin, J. Alcázar, D. W. C. MacMillan, *Science* **2024**, *383*, 1350–1357.
- [51] J. Z. Wang, W. L. Lyon, D. W. C. MacMillan, *Nature* **2024**, *628*, 104–109.
- [52] F. Cong, G.-Q. Sun, S.-H. Ye, R. Hu, W. Rao, M. J. Koh, *J. Am. Chem. Soc.* **2024**, *146*, 10274–10280.
- [53] J. Z. Wang, E. Mao, J. A. Nguyen, W. L. Lyon, D. W. C. MacMillan, *J. Am. Chem. Soc.* **2024**, *146*, 15693–15700.
- [54] J. K. Kochi, *J. Am. Chem. Soc.* **1962**, *84*, 2121–2127.
- [55] P. Lian, W. Long, J. Li, Y. Zheng, X. Wan, *Angew. Chem. Int. Ed.* **2020**, *59*, 23603–23608.
- [56] Y. Tian, X.-T. Li, J.-R. Liu, J. Cheng, A. Gao, N.-Y. Yang, Z. Li, K.-X. Guo, W. Zhang, H.-T. Wen, Z.-L. Li, Q.-S. Gu, X. Hong, X.-Y. Liu, *Nat. Chem.* **2024**, *16*, 466–475.
- [57] K.-J. Bian, D. Nemoto, S.-C. Kao, Y. He, Y. Li, X.-S. Wang, J. G. West, *J. Am. Chem. Soc.* **2022**, *144*, 11810–11821.

Manuscript received: June 3, 2024

Revised manuscript received: July 5, 2024

Accepted manuscript online: August 8, 2024

Version of record online: August 31, 2024